

Characterization of Nano Sized Microstructures in Fe and Ni Base ODS Alloys Using Small Angle Neutron Scattering

Young-Soo Han ^{a*}, Jin-Sung Jang ^b, Xiaodong Mao ^b

^aNeutron Science Division, Korea Atomic Energy Research Institute, 989-111 Daedeok-daero, Yuseong-gu, Daejeon, 305-353

^bNuclear Materials Development Division, Korea Atomic Energy Research Institute, 989-111 Daedeok-daero, Yuseong-gu, Daejeon, 305-353

*Corresponding author: yshan@kaeri.re.kr

1. Introduction

Oxide-dispersion-strengthened (ODS) alloys are the most promising structural materials for future nuclear power systems because of their excellent resistance to both irradiation damage and high-temperature creep. In particular, ferritic ODS alloy is known as a primary candidate material of the cladding tubes of a sodium fast reactor (SFR) in the Generation IV research program. In ODS alloy, the major contribution to the enhanced high-temperature mechanical property comes from the existence of nano-sized oxide precipitates, which act as obstacles to the movement of dislocations. In addition for the extremely high temperature application (>950 °C) of future nuclear system, Ni base ODS alloys are considered as candidate materials. Therefore the characterization of nano-sized microstructures is important for determining the mechanical properties of the material. Small angle neutron scattering (SANS) technique non-destructively probes structures in materials at the nano-meter length of scale (1 - 1000 nm) and has been a very powerful tool in a variety of scientific/engineering research areas.

In this study, nano-sized microstructures were quantitatively analyzed by small angle neutron scattering. The effects of fabrication conditions on the microstructure are discussed in relation to the quantitative analysis results obtained by SANS. The characteristics of the nano-sized oxides in experimental ODS alloys are discussed from the SANS analysis results.

2. Methods and Results

2.1 Experimental Procedures

The Fe base ODS alloy were fabricated by mechanical alloying and hot isostatic pressing processes. The chemical fractions of the Fe base ODS alloy are Fe-12Cr-1.1W-0.2V-0.14Ta-0.3Y₂O₃ in wt %. To reduce the activation in steels used as structural components of reactors, slow-decaying elements such as Nb, Mo and Ni are replaced by others that exhibit a higher decay rate of induced radioactivity such as W and Ta. Elemental metal powders with yttria powder of ~30 nm

in size were mechanically alloyed(MA) by using a Pulverisette-5 planetary ball mill at 200 rpm in an Ar atmosphere for 12 h with a ball to powder ratio of 15:1. The MA powder was then filled into a 304 stainless steel crucible, followed by degassing at 500 °C under 10⁻³ Pa for 1 h and sealing. The MA powder was consolidated at 1150 °C under 100 MPa for 4 h. The hiped bar was then pre-heated at 1200 °C for 2 h and hot rolled into a 15 mm thick plate, which corresponds to a reduction ratio of 50%. For the plate, normalizing heat treatment was performed at 1050 °C for 1 h and tempering was carried out at 750 °C for 2 h. The sample was then isothermally annealed at 1250 °C for 500 h under vacuum. As-hipped, as-hot rolled and heat treated samples of 12Cr ODS alloy were measured by SANS. SANS experiments were carried out using a 40 m SANS instrument at the HANARO reactor at KAERI [1-4].

The two different Ni base ODS alloys were fabricated by mechanical alloying and hot extrusion processes. The chemical compositions of the Ni base ODS alloys are Ni-22Cr-18Fe-1.5Co-9Mo-0.6W-0.8Mn-0.3Si-0.6 Y₂O₃ (Hastelloy XR) and Ni-22Cr-1.5Fe-12.5Co-9Mo-0.3Ti-1Al-0.6 Y₂O₃ (Inconel 617). The mechanical alloying were performed at 200 rpm in an Ar atmosphere for 40 hrs. After the filling of MA powders into a 304 stainless steel crucible and degassing, the hot powder extrusion were applied at two different temperature at 1000 °C, 1100 °C, and 1200 °C

For 12Cr ODS alloys, neutrons of wavelengths = 6 Å and 7.49 Å with a wavelength spread (full width at half maximum) of 12% were used. Three different sample-to-detector distances (SDD = 1.16 m and 5.7 m for λ = 6 Å and SDD = 19.85 m for λ = 7.49 Å) were used. To extend the low q limit, we used a set of refractive focusing lenses for λ = 7.49 Å and SDD = 19.85 m. The 12Cr ODS alloy samples was placed in a saturating magnetic field of 1.2 Tesla perpendicular to a neutron beam direction during SANS experiment. The data perpendicular and parallel to the magnetic field were collected separately with an angular width of 20 degrees from the 2-dimensional SANS data in order to divide the magnetic and nuclear scattering cross sections.

For Ni base ODS alloys, no magnetic field were applied during the experiments. Neutrons of wavelengths = 7.49 Å with a wavelength spread (full

width at half maximum) of 12% were used. Three different sample-to-detector distances (SDD = 1.16 m, 4.7 m and 19.85 m) were used to cover the overall q range of $0.0007 \text{ \AA}^{-1} < q < 0.55 \text{ \AA}^{-1}$.

To obtain quantitative information of the precipitates, the SANS data were fitted assuming that the scatterers were polydisperse spherical particles.

2.2 Fe base ODS alloy

Fig. 1 shows the magnetic SANS intensities of the 12Cr ODS alloy. The bump is shown in the SANS pattern around the scattering vector(Q) range of 0.05 for the as-hipped 12Cr ODS alloy. The bumps shown in the SANS patterns of the as-hot rolled and heat treated 12Cr ODS alloys appeared at around a Q range of lower than 0.05. This result shows that the coarsening of nano sized oxides in the 12Cr ODS alloy occurred after hot rolling and heat treatment. The large-sized Cr_2O_3 contribute to the low Q region, and small-sized YTaO_4 contribute to the high Q region of the SANS pattern. The small sized YTaO_4 ($d \sim 5 \text{ nm}$) exist in the as-hipped 12Cr ODS alloy. It is known that the extraordinary mechanical properties of oxide-dispersion-strengthened alloy originate from highly stabilized oxide nano-clusters with a size smaller than 5 nm.

The average A-ratio of the as-hipped 12Cr ODS alloy is obtained as 2.3, while the theoretical A-ratio is calculated as 4.53. The theoretical A-ratio is about two-times larger than the experimental A-ratio. It is considered that the difference between the theoretical and experimental A-ratios is due to the imperfection in YTaO_4 . When imperfections such as voids are included in YTaO_4 , the A-ratio decreases with an increase in the volume fraction of voids in YTaO_4 . The relationship between the A ratio and volume fraction of voids in the precipitates can be expressed by a simple equation, and the theoretical A-ratio can be calculated with the volume fraction of the voids. If 30% of the voids are included in the YTaO_4 , the A-ratio calculated as 2.3[5].

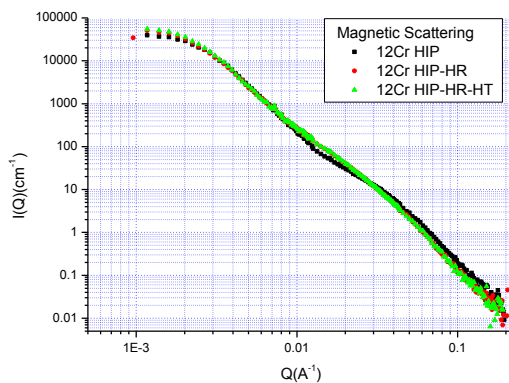


Fig. 1. SANS data of Fe base ODS alloy.

2.3 Ni Base ODS Alloys

Fig. 2 shows the SANS intensities of Ni base ODS alloy with varying the extrusion temperatures. As the hot extrusion temperature increases from 1000°C to 1200°C , the SANS intensity decreases. From the fitting results, it is shown that the volume fraction of the mid-sized particles ($\sim 30 \text{ nm}$) increases rapidly as hot extrusion temperature decreases. The mid sized particles($\sim 30 \text{ nm}$) are identified as γ' phases and small sized particles($< 10 \text{ nm}$) are identified as $\text{Y}_2\text{Ti}_2\text{O}_7$.

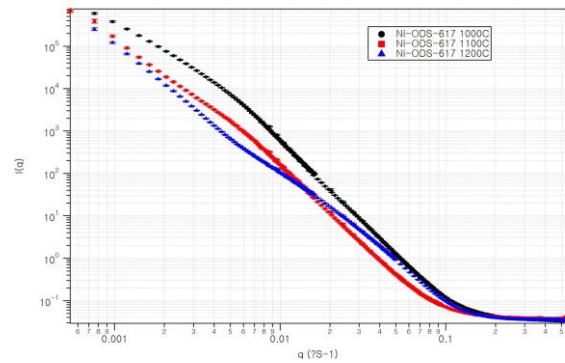


Fig. 2. SANS data of Ni base ODS alloy.

3. Conclusions

Quantitative microstructural information on nano-sized oxide in ODS alloys was obtained from SANS data. The effects of the thermo mechanical treatment on the size and volume fraction of nano-sized oxides were analyzed. For 12Cr ODS alloy, the experimental A-ratio is two-times larger than the theoretical A-ratio., and this result is considered to be due to the imperfections included in YTaO_4 . For Ni base ODS alloy, the volume fraction of the mid-sized particles ($\sim 30 \text{ nm}$) increases rapidly as hot extrusion temperature decreases. The mid sized particles($\sim 30 \text{ nm}$) are identified as γ' phases

REFERENCES

- [1] Y.S. Han, S.M. Choi, T.H. Kim, C.H. Lee and H.R. Kim, Physica B. Vol.1177, p. 385, 2002.
- [2] Y.S. Han, S.M. Choi, T.H. Kim, C.H. Lee and H.R. Kim, J. Appl. Cryst. Vol.40, s442, 2007.
- [3] Y.S. Han, S.M. Choi, T.H. Kim, C.H. Lee, S.J. Cho and B.S. Baek, Nucl. Inst. Meth. Phys. Res. A Vol.721, p.17, 2013.
- [4] S.M. Choi, J.G. Barker, C.J. Glinka, Y.T. Cheong and P.L. Gammel, J. Appl. Cryst. Vol.33, p. 793, 2000.
- [5] Y.S. Han, X. Mao, J.S. Jang and T.K. Kim, Appl. Phys. A Vol. 119, p. 249, 2015